Chapter 3

A setup for direct measurement of adiabatic temperature change in magnetocaloric materials

In this chapter, we discuss a homemade prototype and a measurement setup for the direct measurement of magnetocaloric effect (MCE). The direct adiabatic temperature change (i.e. MCE) is measured on a standard Gadolinium sample.

3.1 Introduction

Refrigeration plays a pivotal role in modern life, significantly improving daily living standards and driving human progress. However, it accounts for over 18% of global energy consumption, and that continues to rise as refrigeration technologies expand in developing regions [1–3]. Currently, nearly a fifth of global electricity use is dedicated to space cooling, with the annual demand exceeding 2000 terawatt-hours (TWh) [4]. The global demand for cooling is projected to increase significantly in the coming years. This growth is driven by rising temperatures due to climate change and factors such as population growth, urbanization, etc. [1]. The increasing energy demand and environmental challenges of traditional gas compression systems underscore the need for new sustainable alternatives and must be consistently upgraded. The gas-compression-based systems used in heating, ventilation, and air conditioning pose several issues. They use excessive energy, have low efficiency, and depend on harmful refrigerants such as chlorofluorocarbon (CFC) and hydrochlorofluorocarbon (HCFC) [5]. These refrigerants contribute to stratospheric ozone depletion and global climate change [6–8]. Magnetic refrigeration stands out as a promising solution with its high efficiency and lower electricity consumption [9–11]. Magnetic refrigeration depends on the magnetocaloric effect (MCE), which induces either an adiabatic temperature change (ΔT_{ad}) or an isothermal entropy change (ΔS_{iso}) in magnetic materials when the magnetic field is altered [12, 13]. As shown in Figs. 3.1(a,b), the MCE-based technique is among the most efficient solid-state caloric methods, alongside the elastocaloric (eCE), barocaloric (BCE), and electrocaloric (ECE) techniques [14, 15]. This approach can achieve energy efficiencies above 60%, far surpassing the ∼40% Carnot efficiency of leading commercial gas-compression-based systems [5]. Furthermore, magnetocaloric systems are a sustainable technology, as they avoid the use of hazardous refrigerants such as HCFC during operation. Similarly to the gas compres-

sion cycle, a refrigerant cycle also operates by cyclically varying the magnetic field [15]. A magnetic cooling system consists of four key elements: a magnetocaloric (MC) material, a magnetic field source, a mechanism to move the material or switch the field on/off, and a heat exchanger. Although MCE was discovered in 1881, significant progress was made in 1997 when Pecharsky and Gschneidner identified an intermetallic Gd-Si-Ge material that exhibited a substantial ΔT_{ad} near room temperature. This material was identified as demonstrating a giant magnetocaloric effect [16]. MCE is a material property that arises from spin-phonon interactions. Under adiabatic conditions, the total entropy of the material (phonon and magnetic contributions) remains conserved. The application or removal of a magnetic field alters the magnetic entropy, causing a corresponding change in phonon entropy and the temperature of materials. The temperature change depends on the properties of materials and the strength of the applied magnetic field. This direct measurement of ΔT_{ad} helps evaluate the cooling efficiency of MC. ΔS_{iso} can be calculated using isothermal magnetization measurements as a function of the field and it can be used to estimate ΔT_{ad} when combined with temperature and field-dependent heat capacity (C_H) measurements. This is the indirect method to determine the MCE. This approach is well-known, and instruments for magnetization and heat capacity measurements are widely available. As a result, indirect measurements of the MCE are commonly reported. Pecharsky et al. evaluated the error associated with this method and found that it can reach approximately 15% for pure Gd [17]. Indirect measurements are often preferred for their accessibility despite the potential inaccuracies. To measure ΔT_{ad} directly, an experiment setup is needed to record the temperature change under adiabatic conditions when the magnetic field is altered. Although many prototypes of magnetic refrigerators have been developed over the past two decades, creating competitive magnetocaloric devices still requires better-performing MC materials and innovative technical solutions [13, 15, 18]. In addition to basic research on the magnetic properties of materials, finding efficient cooling elements necessitates measuring their MC performance. In this regard, experimental setups have been designed where the sample temperature is typically measured using standard temperature sensors such as thermocouples [19–26] or high-precision thermoresistances [27, 28].

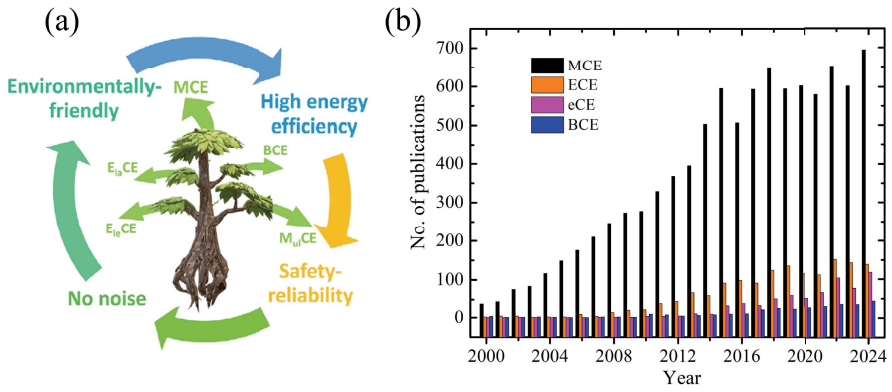

Figure 3.1: (a) Typical solid-state caloric energy conversion and its advantages compared with traditional vapour-compression technique [8]. (b) Research publications for different caloric effects from 2000 to 2024 (data taken from scopus journal).

The magnetic field change is usually achieved by switching an electromagnet or superconducting magnet on and off [19, 23, 25, 28, 29], moving the sample relative to a field source [20, 26–28], or by using pulsed magnetic fields [19, 22, 30, 31]. Although this procedure appears straight forward but the ΔT_{ad} is less frequently reported in the literature compared to ΔS_{iso}. This is primarily because suitable commercial instruments are not readily available.

This chapter introduces a prototype utilizing a permanent magnet and a measurement setup with an electromagnet, both designed to measure the direct ΔT_{ad}. The prototype demonstrates how permanent magnets can generate the required magnetic field variation by moving the magnet closer to the sample and determine the direct ΔT_{ad}. The electromagnet-based setup ensures precise control of the magnetic field for accurate measurements. Together, these systems provide a practical approach for studying the MCE under controlled conditions. The real-time data was recorded using the LabView program.

3.2 Experimental setup

MCE can be measured using two experimental approaches: (1) direct measurement of ΔT_{ad}, and (2) indirect estimation by isothermal ΔS_{iso} (discussed in detail in Chapter 1). In direct MCE measurements, the sample can be exposed to the magnetic field in two ways: (a) by keeping the magnet stationary while moving the sample in and out of the magnetic field or (b) by fixing the sample and changing the magnetic field. Here, in this

study, a prototype using a permanent magnet is developed to measure direct ΔT_{ad} at room temperature. A direct ΔT_{ad} measurement setup based on electromagnet is also designed, which measures the direct ΔT_{ad} from ambient temperature to 100 K. In these setups, a polycrystalline Gd with 99.9% purity is used as a MC material (obtained from a commercial source). Real-time temperature data is recorded using a Lakeshore temperature controller. The temperature sensor is placed directly on the Gd sample to reduce ambient effect. This arrangement of sensor allows for more accurate data, as the measured temperature changes are directly related to the physical behavior of materials in the magnetic field [32]. Most of the reported direct adiabatic temperature measurement setups use thermocouples to measure the temperature [33–35]. In this work, a PT100 temperature sensor is used instead, as thermocouple readings can be disturbed by varying magnetic fields. The PT100 sensor is preferred for its low magnetic field-induced errors and affordability. The minimal thermal losses also make it possible to measure MCE using samples with a mass of $\sim$10 mg.

3.2.1 Prototype using permanent magnet

For direct measurement of ΔT_{ad}, a measurement system should have three important elements (1) a temperature sensor/thermometer to measure the sample temperature over time; (2) a magnetic field source or a permanent magnet with a mechanical machine to move the sample in and out of the magnetic field; (3) a sample holder with a temperature sensor, which can maintain adiabatic condition. The real image of the prototype is shown in Fig. 3.2(a). In the prototype, a 0.5 T permanent magnet is placed in a non-magnetic stainless steel jacket, which is suspended on a screw rod. This screw rod is connected to a 250-watt DC motor and is designed to enable the magnet to achieve maximum linear speed. This design increases the frequency at which the magnetic field can be applied to and removed from the sample. The actual image of the sample holder is shown in Fig. 3.2(b). It is constructed from teflon to reduce heat loss via conduction and features ϕ11 mm diameter hole for sample placement. The Gd sample is mounted inside the sample holder with a PT100 sensor and positioned at the center of the holder. Inset (i) of Fig. 3.2(b) shows a zoomed

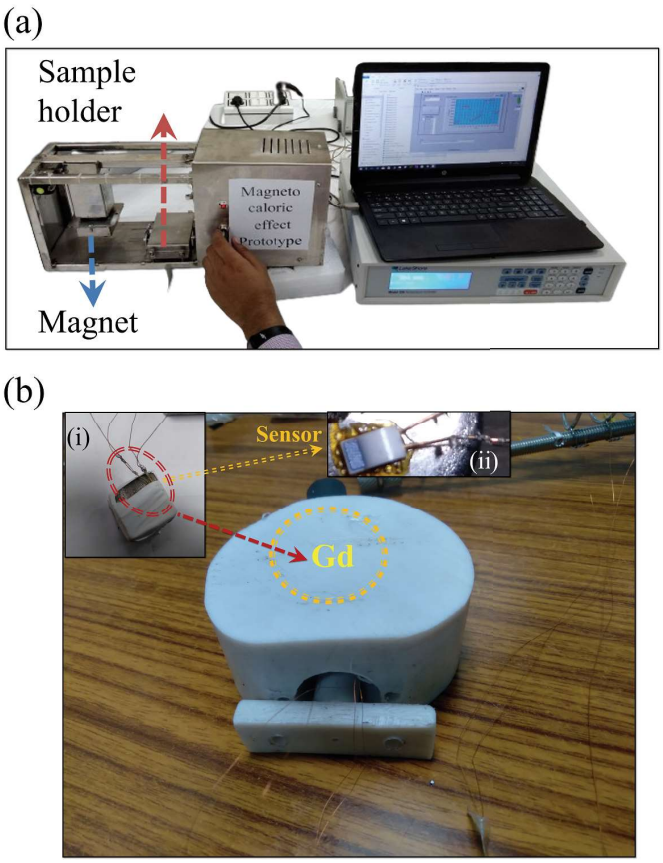

Figure 3.2: (a) Real image of the prototype. (b) Real image of the sample holder. Insets show a magnified view of the Gd sample with the sensor.

view of the sample, while inset (ii) displays the PT100 sensor glued with GE varnish to ensure good thermal contact between the sample and the sensor. This setup helps minimize errors during temperature measurements. The four-probe connecting wires are connected to the temperature controller, which reads the real-time temperature. The temperature readings from the controller are recorded directly and plotted as a function of time using the LabVIEW program. The prototype directly measures ΔT_{ad} near room temperature. In this design, a fixed sample method is used, while a permanent magnet is periodically moved to vary the magnetic field.

3.2.2 MCE Measurement setup using electromagnet

The real image of the measurement setup is shown in Fig. 3.3. It consists of an electromagnet with a magnetic power supply capable of generating a 1 T magnetic field at the center of the magnet bore. The sample holder can be inserted inside the bore. The

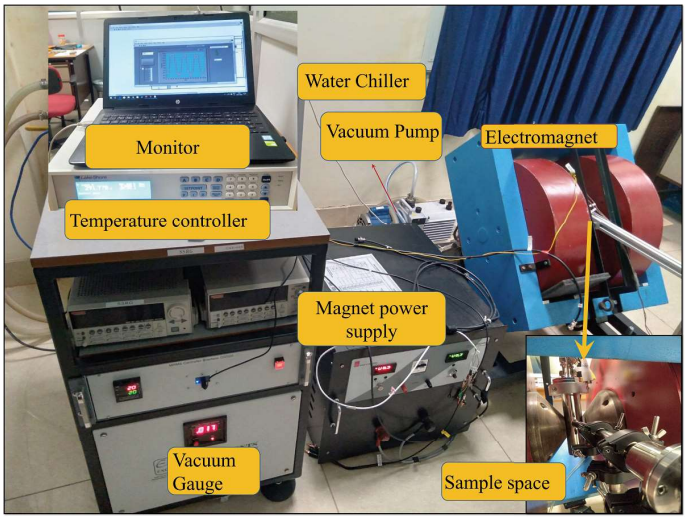

Figure 3.3: Real image of the MCE measurement set up. Inset shows a zoomed view of the sample space in the bore of the electromagnet.

magnetic field is applied by varying the current in the electromagnet coil using a power supply. This allows the magnetic field to be applied to the sample in a controlled and variable manner. The sample holder is enclosed in a stainless steel cylinder, where a vacuum can be created up to 10^{-3} mbar using a rotary pump. The evacuated cylinder is necessary to maintain adiabatic conditions, which minimize heat exchange between the sample and its surroundings during the application or removal of the magnetic field. However, achieving complete thermal insulation contradicts the requirement to control, stabilize, and adjust the sample temperature before measuring ΔT_{ad}. A balance must be found between these opposing requirements. Alternatively, heat dissipation can be minimized by performing rapid measurements using fast magnetic field changes. The actual image of the sample holder is shown in Fig. 3.4. It is equipped with a spiral heater designed to create a uniform temperature environment (up to 100 K), depending on the experimental conditions. A type K thermocouple is used to measure the temperature of the sample environment. The Gd sample is placed at the center of the spiral heater and sample holder, as shown in the inset of Fig. 3.4. To minimize heat loss through the sample holder, Gd is suspended using a teflon thread, and a PT100 sensor is directly glued to the surface of the Gd to ensure good thermal contact with the sample. Using this setup, the direct MCE can be measured at room temperature as well as at higher temperatures up to 100 K for both small and large samples. It is cost-effective and can be easily assembled in a laboratory,

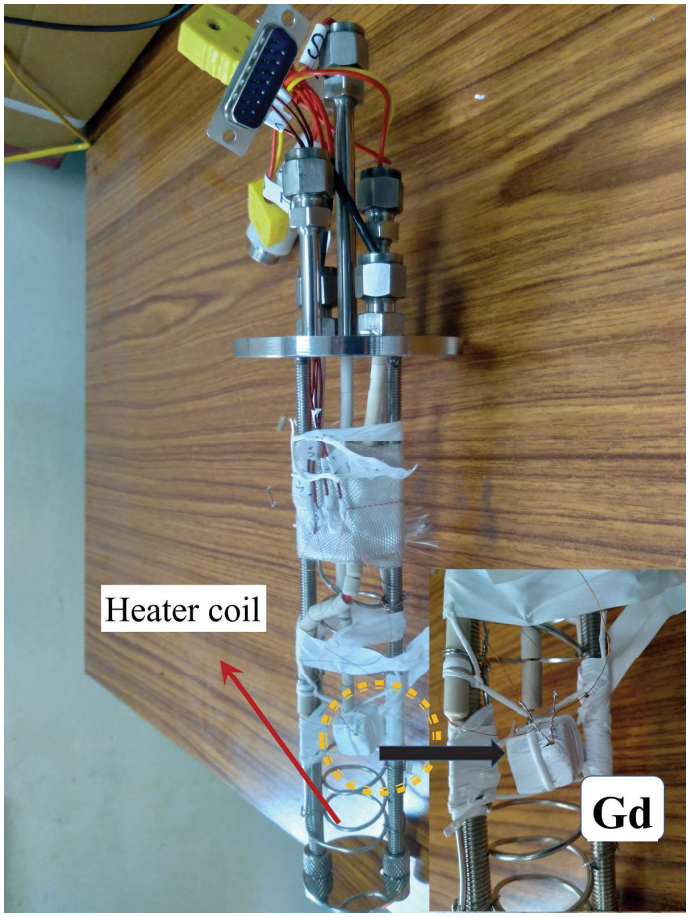

Figure 3.4: Real image of the sample holder. Inset shows the zoomed view of the sample and sensor inside the heater coil.

facilitating research on the development of MC.

3.3 Measurement process and results

The measurement process for the ΔT_{ad} in the prototype setup is illustrated as a pictorial representation in Fig. 3.5(a). This diagram provides a clear visual representation of how the temperature of the sample is monitored during the application or removal of the magnetic field. In Fig. 3.5(a), step (i) shows the initial position of the magnet and sample, where the magnet is far from the sample and the sample remains at room temperature. As the magnet moves towards the sample quickly, using the screw rod and motor arrangement, the temperature of the sample begins to rise [step (ii)]. This increase in temperature is a result of the application of the magnetic field. Afterward, the sample and magnet remain in the same position for 30 seconds to allow for thermal relaxation [step (iii)]. During this

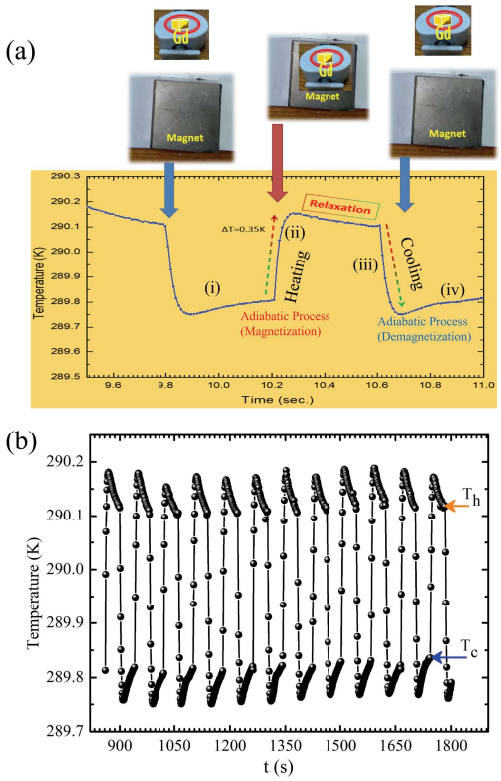

Figure 3.5: (a) Magnetocaloric effect measurement process. (b) Adiabatic temperature change as a function of time measured in prototype for a number of field cycles.

time, the sample temperature stabilizes. Finally, in step (iv), the magnet is moved away from the sample, causing the temperature of the sample to decrease and return to its initial value. The data measured on pure Gd using the MCE prototype is shown in Fig. 3.5(b) for several magnetic field cycles. T_c represents the temperature when the magnetic field is applied to the sample, and T_h represents the temperature when the magnetic field is removed from the sample. The direct ΔT_{ad} is measured to be $\sim$ 0.35 K under a magnetic field of 0.24 T.

The measurement process of ΔT_{ad} in the MCE measurement setup using an electromagnet is shown as a flowchart in Fig. 3.6. The experiment begins by setting the temperature to room temperature (300 K) and the magnetic field to 0 Oe to ensure the sample is in its initial state. Next, the temperature is set to a desired value T_i (near the transition temperature) using a heater. This temperature is maintained constant by the heater coil inside the sample holder during the experiment, meaning the initial sample temperature is T_i (in the present study, the initial sample temperature is ambient temperature). The magnetic field is then

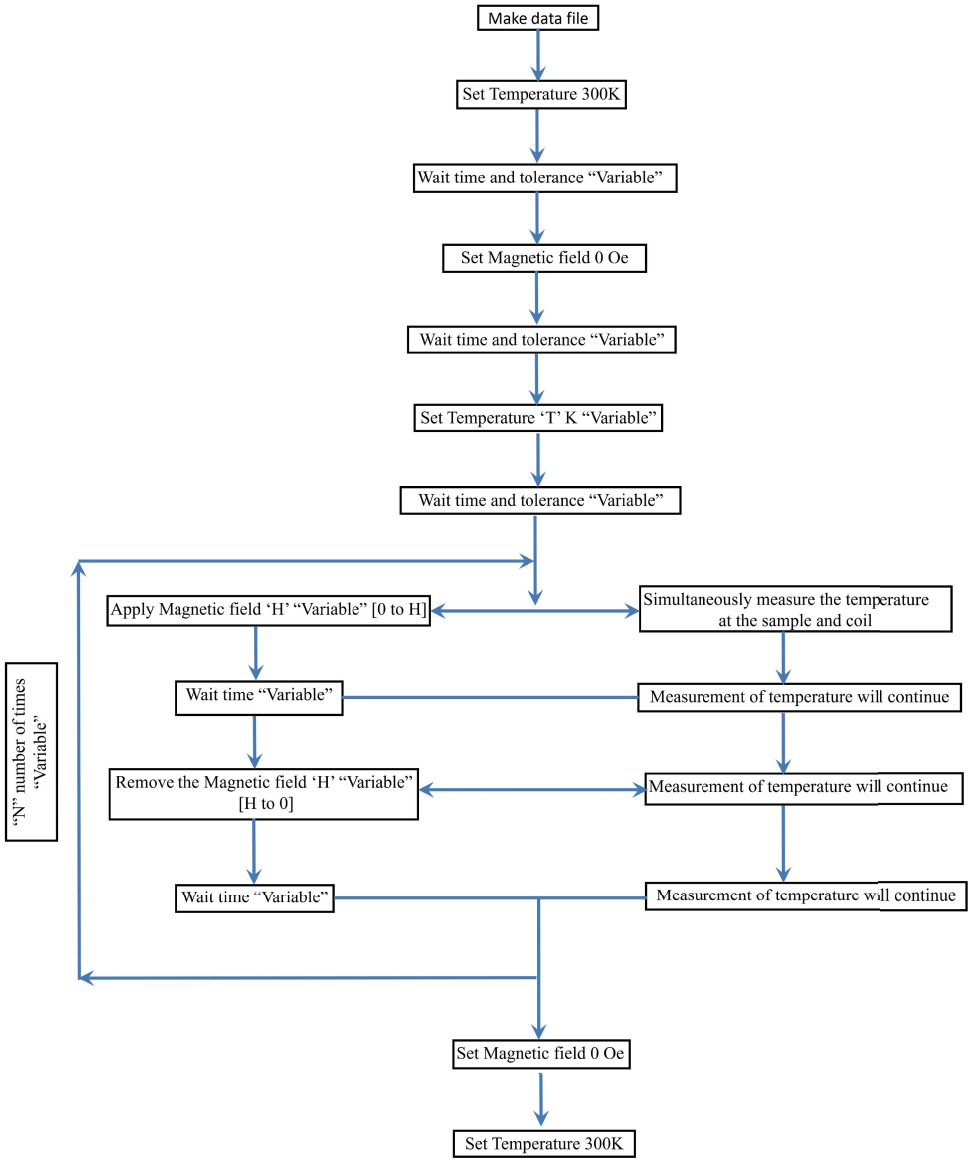

Figure 3.6: Flow chart of the measurement steps in the magnetocaloric effect measurement setup.

applied using a computer-controlled electromagnet power supply. As the magnetic field changes within the bore of the magnet, the temperature of the sample starts to increase and is continuously measured by the attached PT100 temperature sensors. This setup measures both the temperature change and the magnetic field in real time during the application and removal of the magnetic field. A Lakeshore temperature controller is used to record the temperature from the temperature sensor. The experiment proceeds by repeating these four steps multiple times during each magnetic field cycle. Fig. 3.7 shows the MCE data measured over several magnetic field cycles. The estimated value of the ΔT_{ad} is $\sim$ 1.6 K at a 0.9 T magnetic field. Recently, ΔT_{ad} was reported for a pure polycrystalline Gd

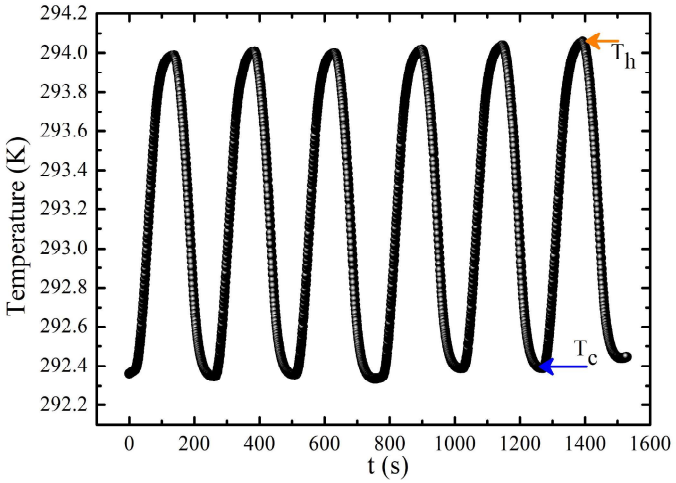

Figure 3.7: Adiabatic temperature change as a function of time measured in magnetocaloric effect measurement set up for a number of field cycle.

sample. Depending on the measurement method and the purity of the sample, the reported values range from 9 to 12 K for a magnetic field of 5 T [19, 20, 36, 37]. Kuz'min et al. reported ΔT_{ad} = 10.1 K for a field span of 4.7 T [33]. For a single crystal of Gd, ΔT_{ad} = 9.5 K was reported when the magnetic field was aligned parallel to the [10$\bar{1}$0] direction. Our measured values of ΔT_{ad} for the polycrystalline Gd sample agree well with these results, using both the prototype and the measurement setup.

3.4 Conclusion

In this work, a simple prototype using a permanent magnet is designed to measure the direct ΔT_{ad} at room temperature. A homemade measurement setup using an electromagnet is also prepared to measure direct MCE in the temperature range from ambient temperature to 100 K. Both setups use a PT100 temperature sensor to measure the temperature change because of its accuracy in magnetic fields and low thermal losses. The prototype measures $\Delta T_{ad} \sim 0.35$ K at 0.24 T magnetic field span, while the MCE measurement setup measures $\sim$1.6 K at 0.9 T field for standard Gd material. These setups are cost-effective and can be easily prepared in the laboratory to enhance research in the development of magnetocaloric materials.

References

[1] T. Peters and L. Sayin, "Future-proofing sustainable cooling demand," tech. rep., ADBI Working Paper, 2022.

[2] F. Cugini and M. Solzi, "On the direct measurement of the adiabatic temperature change of magnetocaloric materials," *J. Appl. Phys.*, vol. 127, no. 12, 2020.

[3] P. Spoonley, "Technological and social changes into the third millennium and the impact on refrigeration," *Int. J. Refrig.*, vol. 24, no. 7, pp. 593–601, 2001.

[4] E. IEA and K. Fikiin, *The Future of Cooling: Opportunities for energy efficient air conditioning*. 05 2018.

[5] J. Lyubina, "Magnetocaloric materials for energy efficient cooling," *J. Phys. D: Appl. Phys.*, vol. 50, no. 5, p. 053002, 2017.

[6] O. BULKOT and L. ANISIMOVA, "Investing in renewable energy transition as a key trend in the global economy," *B I C НИ К*, vol. 2, 2023.

[7] P. Patel and O. Gutfleisch, "Advanced magnetic materials could drive next-generation energy technologies," 2018.

[8] F. Zhang, X. Miao, N. van Dijk, E. Brück, and Y. Ren, "Advanced magnetocaloric materials for energy conversion: Recent progress, opportunities, and perspective," *Adv. Energy Mater.*, p. 2400369, 2024.

[9] K. A. Gschneidner, V. Pecharsky, and A. Tsokol, "Recent developments in magnetocaloric materials," *Rep. Prog. Phys.*, vol. 68, no. 6, p. 1479, 2005.

[10] C. Aprea, A. Greco, A. Maiorino, and C. Masselli, "Magnetic refrigeration: an eco-friendly technology for the refrigeration at room temperature," in *J. Phys. Conf. Ser.*, vol. 655, p. 012026, IOP Publishing, 2015.

[11] E. Brück, "Developments in magnetocaloric refrigeration," *J. Phys. D: Appl. Phys.*, vol. 38, no. 23, p. R381, 2005.

[12] A. M. Tishin and Y. I. Spichkin, *The magnetocaloric effect and its applications*. CRC Press, 2016.

[13] T. Gottschall, K. P. Skokov, M. Fries, A. Taubel, I. Radulov, F. Scheibel, D. Benke, S. Riegg, and O. Gutfleisch, "Making a cool choice: the materials library of magnetic refrigeration," *Adv. Energy Mater.*, vol. 9, no. 34, p. 1901322, 2019.

[14] J. Li, A. Torelló, V. Kovacova, U. Prah, A. Aravindhan, T. Granzow, T. Usui, S. Hirose, and E. Defay, "High cooling performance in a double-loop electrocaloric heat pump," *Sci.*, vol. 382, no. 6672, pp. 801–805, 2023.

[15] A. Kitanovski, J. Tušek, U. Tomc, U. Plaznik, M. Ožbolt, and A. Poredoš, "Magnetocaloric energy conversion," *Green Energy Technol.*, vol. 179, 2015.

[16] V. K. Pecharsky and K. A. Gschneidner Jr, "Giant magnetocaloric effect in $Gd_5(Si_2Ge_2)$," *Phys. Rev. Lett.*, vol. 78, no. 23, p. 4494, 1997.

[17] V. Pecharsky and K. Gschneidner, "J.(1997). giant magnetocaloric effect in $Gd_{5s}Si_2Ge_{2d}$," *Phys. Rev. Lett.*, pp. 4494–4497.

[18] B. Yu, M. Liu, P. W. Egolf, and A. Kitanovski, "A review of magnetic refrigerator and heat pump prototypes built before the year 2010," *Int. J. Refrig.*, vol. 33, no. 6, pp. 1029–1060, 2010.

[19] S. Y. Dan'kov, A. Tishin, V. Pecharsky, and K. Gschneidner, "Experimental device for studying the magnetocaloric effect in pulse magnetic fields," *Rev. Sci. Instrum.*, vol. 68, no. 6, pp. 2432–2437, 1997.

[20] J. Kamarád, J. Kaštil, and Z. Arnold, "Practical system for the direct measurement of magneto-caloric effect by micro-thermocouples," *Rev. Sci. Instrum.*, vol. 83, no. 8, 2012.

[21] X. Moya, L. Mañosa, A. Planes, S. Aksoy, M. Acet, E. F. Wassermann, and T. Krenke, "Cooling and heating by adiabatic magnetization in the $Ni_{50}Mn_{34}In_{16}$ magnetic shape-memory alloy," *Phys. Rev. B*, vol. 75, no. 18, p. 184412, 2007.

[22] M. Ghorbani Zavareh, C. Salazar Mejía, A. Nayak, Y. Skourski, J. Wosnitza, C. Felser, and M. Nicklas, "Direct measurements of the magnetocaloric effect in pulsed magnetic fields: The example of the Heusler alloy $Ni_{50}Mn_{35}In_{15}$," *Appl. Phys. Lett.*, vol. 106, no. 7, 2015.

[23] S. Benford and G. Brown, "T-S diagram for gadolinium near the Curie temperature," *J. Appl. Phys.*, vol. 52, no. 3, pp. 2110–2112, 1981.

[24] K. Skokov, V. Khovaylo, K.-H. Müller, J. Moore, J. Liu, and O. Gutfleisch, "Magnetocaloric materials with first-order phase transition: thermal and magnetic hysteresis in $LaFe_{11.8}Si_{1.2}$ and $Ni_{2.21}Mn_{0.77}Ga_{1.02}$," *J. Appl. Phys.*, vol. 111, no. 7, 2012.

[25] F. Canepa, S. Cirafici, M. Napoletano, C. Ciccarelli, and C. Belfortini, "Direct measurement of the magnetocaloric effect of microstructured Gd eutectic compounds using a new fast automatic device," *Solid State Commun.*, vol. 133, no. 4, pp. 241–244, 2005.

[26] A. Aliev, A. Batdalov, L. Khanov, V. Koledov, V. Shavrov, I. Tereshina, and S. Taskaev, "Magnetocaloric effect in some magnetic materials in alternating magnetic fields up to 22 Hz," *J. Alloys Compd.*, vol. 676, pp. 601–605, 2016.

[27] B. Gopal, R. Chahine, and T. Bose, "A sample translatory type insert for automated magnetocaloric effect measurements," *Rev. Sci. Instrum.*, vol. 68, no. 4, pp. 1818–1822, 1997.

[28] G. Porcari, M. Buzzi, F. Cugini, R. Pellicelli, C. Pernechele, L. Caron, E. Brück, and M. Solzi, "Direct magnetocaloric characterization and simulation of thermomagnetic cycles," *Rev. Sci. Instrum.*, vol. 84, no. 7, 2013.

[29] F. Cugini, G. Porcari, and M. Solzi, "Non-contact direct measurement of the magnetocaloric effect in thin samples," *Rev. Sci. Instrum.*, vol. 85, no. 7, 2014.

[30] T. Kihara, Y. Kohama, Y. Hashimoto, S. Katsumoto, and M. Tokunaga, "Adiabatic measurements of magneto-caloric effects in pulsed high magnetic fields up to 55T," *Rev. Sci. Instrum.*, vol. 84, no. 7, 2013.

[31] F. Cugini, G. Porcari, C. Viappiani, L. Caron, A. Dos Santos, L. Cardoso, E. Passamani, J. Proveti, S. Gama, E. Brück, *et al.*, "Millisecond direct measurement of the magnetocaloric effect of a Fe_2P-based compound by the mirage effect," *Appl. Phys. Lett.*, vol. 108, no. 1, 2016.

[32] W. Boettinger, U. Kattner, K. Moon, and J. Perepezko, "DTA and heat-flux DSC measurements of alloy melting and freezing: Nist recommended practice guide, special publication 960-15," *National Institute of Standards and Technology, Washington, DC, USA*, 2006.

[33] M. Kuz'min, K. Skokov, D. Y. Karpenkov, J. Moore, M. Richter, and O. Gutfleisch, "Magnetic field dependence of the maximum adiabatic temperature change," *Appl. Phys. Lett.*, vol. 99, no. 1, 2011.

[34] V. Franco, A. Conde, J. Romero-Enrique, Y. Spichkin, V. Zverev, and A. Tishin, "Field dependence of the adiabatic temperature change in second order phase transition materials: Application to Gd," *J. Appl. Phys.*, vol. 106, no. 10, 2009.

[35] Y. I. Spichkin, A. Derkach, A. Tishin, M. Kuz'min, A. Chernyshov, K. Gschneidner Jr, and V. Pecharsky, "Thermodynamic features of magnetization and magnetocaloric effect near the magnetic ordering temperature of Gd," *J. Magn. Magn. Mater.*, vol. 316, no. 2, pp. e555–e557, 2007.

[36] A. Tishin, K. Gschneidner Jr, and V. Pecharsky, "Magnetocaloric effect and heat capacity in the phase-transition region," *Phys. Rev. B.*, vol. 59, no. 1, p. 503, 1999.

[37] K. Gschneidner Jr and V. K. Pecharsky, "Magnetocaloric materials," *Annu. Rev. Mater. Sci.*, vol. 30, no. 1, pp. 387–429, 2000.